# EPR Spin-trapping Studies of the Reaction of the Hydroxyl Radical with Pyrimidine Nucleobases, Nucleosides and Nucleotides, Polynucleotides, and RNA. Direct Evidence for Sites of Initial Attack and for Strand Breakage

**Helen Catterall, Michael J. Davies, Bruce C. Gilbert* and Natalie P. Polack**
*Department of Chemistry, University of York, Heslington, York, UK YO1 5DD*

Spin-trapping experiments with the trap $Me_3CNO$ have been employed to identify the radicals formed by reaction of ·OH (generated from reaction of $H_2O_2$ with a variety of transition-metal ions) with pyrimidine derivatives relevant to nucleic acids. Results for the nucleobases, nucleosides and nucleotides confirm the predominance of attack at the C5 and C6 carbon atoms in the pyrimidine ring. Evidence for subsequent transfer is derived from experiments with poly(U) and other polynucleotides as well as RNA, in which anisotropic spectra from immobilized nitroxide adducts can be distinguished from sharper, isotropic spectra which result from further radical damage [pH dependent for poly(U)] or enzymatic cleavage.

A variety of techniques, including pulse radiolysis with optical and conductivity detection,[1,2] EPR spectroscopy with continuous-flow and spin-trapping,[3-8] and product studies[9-11] have been employed to study the reactions of ·OH with nucleic acids and their components and, in particular, the ways in which strand-breakage (involving sugar–phosphate bond fission) may follow radical attack. It is well established that attack of ·OH on pyrimidine nucleosides and nucleotides occurs predominantly *via* addition of ·OH to the C5–C6 double bond in the base moiety, with a relatively small extent of hydrogen-atom abstraction from the sugar.[12] However, the mechanism of transfer of the site of radical attack on the pyrimidine to the sugar ring, as a prelude to fragmentation *via* phosphate loss, is not clear, though under certain circumstances peroxyl radicals or radical-cations may be involved: we have shown, for example, how protonation of ·OH adducts leads to cation-radical formation and rapid transfer of the radical centre to C2′ (at least) in the ribose ring in uridine and cytidine.[13]

In the investigation to be described here we set out to develop small-scale spin-trapping approaches in order to detect first-formed radicals in the reaction of ·OH (from metal–hydrogen peroxide couples) with polynucleotides [*e.g.*, poly(U)] and nucleic acids (RNA) as well as simple analogues. Our aim was to characterize clearly the spin-adducts (of $Me_3CNO$, MNP) of radicals formed not only by addition and abstraction but also by subsequent reactions involving damage-transfer and chain-fragmentation (strand-breakage).

## Results and Discussion

(*a*) *Reactions of Pyrimidine Nucleobases, Nucleosides and Nucleotides.*—Most of our experiments with these substrates involved reaction of the nucleobase (or derivative) with the $Ti^{III}$–$H_2O_2$ couple as a source of the hydroxyl radical. The experiments typically involved recording EPR spectra for a period of time (up to 2 h), commencing shortly after mixing the solutions and transfer to an aqueous solution sample cell: concentrations employed were generally (after mixing) [$Ti^{III}$] $3 \times 10^{-4}$ mol $dm^{-3}$, [$H_2O_2$] $7 \times 10^{-3}$ mol $dm^{-3}$, [MNP] in the range $0.5 \times 10^{-2}$ to $2 \times 10^{-2}$ mol $dm^{-3}$, with the substrate in excess and the pH in the range 1–9. Solutions were normally deoxygenated by purging with nitrogen. Experiments were also carried out with the $Fe^{II}$–$H_2O_2$ couple, which is also believed to be a source of ·OH; these were found to give slightly weaker, though essentially similar, EPR signals. For the bases, nucleosides and nucleotides, the $Ti^{III}$–$H_2O_2$ system was generally the method of choice.

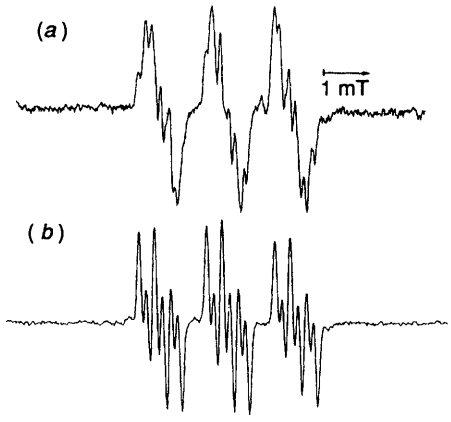


**Fig. 1** EPR spectra of spin adducts **2** and **3** formed from the addition of the C5- and C6-hydroxyl adducts of uracil to MNP; obtained from the reaction of $Ti^{III}$ ($3 \times 10^{-4}$ mol $dm^{-3}$) and $H_2O_2$ ($7 \times 10^{-3}$ mol $dm^{-3}$) with uracil (0.03 mol $dm^{-3}$) in the presence of MNP at (*a*) pH 7 and (*b*) pH 2. The C5-adduct is dominant for the latter conditions.

(*i*) *Nucleobases.* The suggestion that ·OH reacts with uracil (**1**) to give the C5- and C6-hydroxyl adducts (in the ratio 4:1 respectively) is supported by the observation of two spin-adducts at pH 7 (Table 1): the major radical **2**, with a clearly defined β-nitrogen splitting is more clearly revealed in experiments at low pH in which it is the dominant species detected (see Fig. 1). The disappearance of **3** at low pH is believed to reflect the ease of reduction of the C6-adduct (the 5-yl radical) by $Ti^{III}$–EDTA at low pH [reactions (1) and (2)].[3]

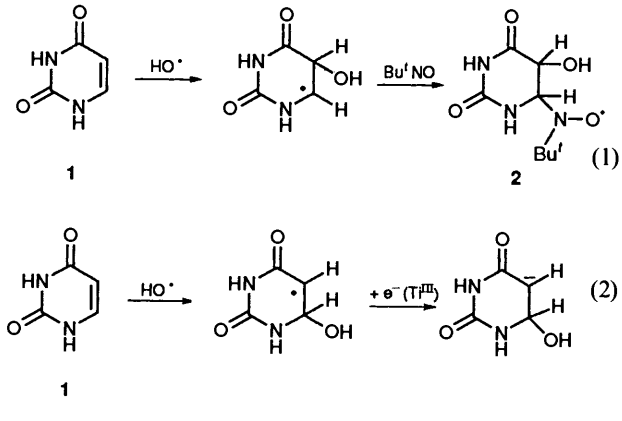

In related experiments with cytosine (**4**) the two corresponding adducts were also obtained with the C5-adduct (**5**) clearly dominant (the parameters of the C6-hydroxyl adduct can only be estimated): minor changes as a function of pH may reflect the removal of the precursor to **6** or changes in EPR parameters on protonation (protonated cytosine has p$K$ 4.5).[14]

With 1-methylcytosine (**7**) clear signals were obtained from the spin-trapped C5-OH adduct (the C6-yl radical, **8**) the spectra of which, again dominated by a β-nitrogen splitting, are clearly different at high and low pH, corresponding to the effects of protonation of the amino group on the spectra (see Fig. 2). The β-nitrogen and -proton splittings are clearly very sensitive to the state of protonation, which in turn evidently affects the preferred conformation. Comparison of parameters for **2**, **5**, **8**, **9** and other related species [*e.g.*, **11**; see later] indicate that $a$(N) and $a$(H) change in opposite directions with changes in

**Table 1** EPR parameters for aminoxyls obtained by spin-trapping radicals from ·OH and pyrimidine derivatives in the presence of MNP

| Substrate | Radical(s) | pH | Hyperfine splittings $a$(α-N)[a] | $a$(β-H)[a] | $a$(other)[a] |
|---|---|---|---|---|---|
| 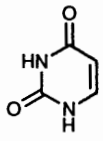 **1** | 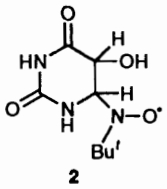 **2** | 1–9 | 1.50 | 0.16 | 0.35 (β-N) |
| | 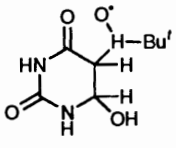 **3** | 7–9 | 1.37[b] | 0.42[b] | — |
| 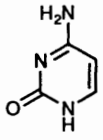 **4** | 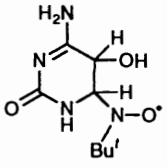 **5** | 1–9 | 1.49[c] | 0.15[c] | 0.35 (β-N)<br>0.02 (γ-H) |
| | 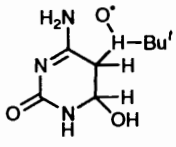 **6** | 1–9 | 1.53[b,c] | 0.32[b,c] | |
| 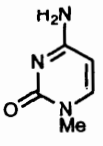 **7** | 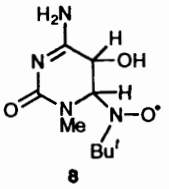 **8** | 4–9 | 1.49 | 0.21 | 0.21 (β-N) |
| | 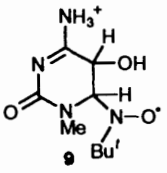 **9** | 1–4 | 1.51 | 0.41 | 0.14 (β-N)<br>0.05 (γ-H) |
| 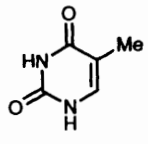 **10** | 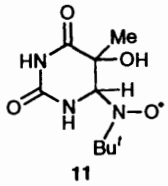 **11** | 1–9 | 1.51 | — | 0.35 (β-N) |
| | 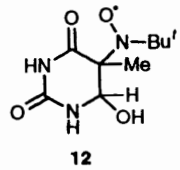 **12** | 7–9 | 1.55 | — | — |

**Table 1** (*continued*)

| Substrate | Radical(s) | pH | Hyperfine splittings $a(\alpha\text{-N})^a$ | $a(\beta\text{-H})^a$ | $a(\text{other})^a$ |
|---|---|---|---|---|---|
| | 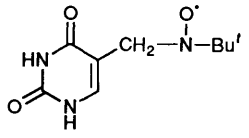 **13** | ≥ 10 | *ca.* 1.5 | *ca.* 0.60 | |
| 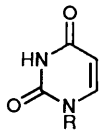 **14**[d] | 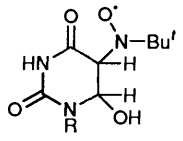 **15**[d] | 1–9 | 1.51 | 0.35 | |
| | 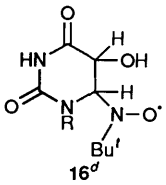 **16**[d] | 1–9 | 1.50 | 0.68 | |
| | —[e] | < 1 | 1.57 | 0.13 | |
| | 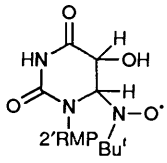 **18**[f] | 1–9 | 1.53 | 0.73 | |
| 2′UMP **17**[f] | | | | | |
| | 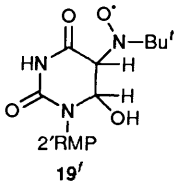 **19**[f] | 1–9 | 1.53 | 0.40 | |
| | 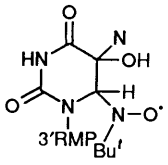 **21**[f] | 1–9 | 1.48 | 0.72 | |
| 3′UMP **20**[f] | | | | | |
| | 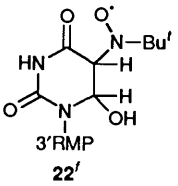 **22**[f] | 1–9 | 1.49 | 0.36 | |
| | 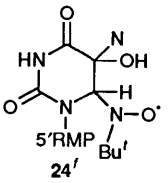 **24**[f] | 1–9 | 1.51 | 0.72 | |
| 5′UMP **23**[f] | | | | | |
| |  **25**[f] | 1–9 | 1.53 | 0.37 | |

**Table 1** (*continued*)

| Substrate | Radical(s) | pH | Hyperfine splittings $a$(α-N)[a] | $a$(β-H)[a] | $a$(other)[a] |
|---|---|---|---|---|---|
| | —[e] | < 1 | 1.49 | 0.10 | |
| 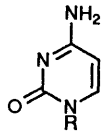 26[d] | 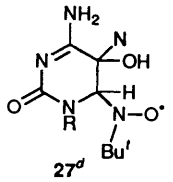 27[d] | 1–9 | 1.48[c] | 0.65[c] | |
| | 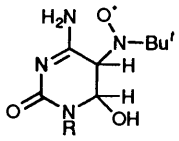 28[d] | 1–9 | 1.49[c] | 0.38[c] | |
| 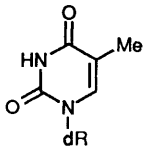 29[g] | 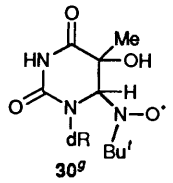 30[g] | 1–9 | 1.43 | | 0.30 (β-N) |
| | 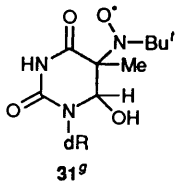 31[g] | 1–9 | 1.60 | | |

[a] Typically ± 0.005 mT, except where indicated otherwise; $g$ = 2.0059 ± 0.0001. [b] Estimated parameters: see the text. [c] Parameters measured at pH *ca.* 7; minor variation noted at lower pH, where the amino group will be protonated. [d] R = ribose. [e] Spectra at low pH may be from sugar derived radicals. [f] RMP = monophosphate of ribose. [g] R = 2′-deoxyribose.

substitution. We expect both splittings to be governed by a $B\cos^2\theta$ type relationship (where $\theta$ is the appropriate dihedral angle), so the behaviour is understandable.

With thymine **10**, reaction with •OH led to the detection of signals assigned to the C5-OH adduct **11** throughout the pH range 1–9: the β-nitrogen splitting is again dominant (the β-proton splitting is presumably lost within the line-width). At higher pH values (see Fig. 3), the extra signal detected, with a major nitrogen triplet but no further splitting, is attributed to the C6-OH adduct **12**: we believe that it is readily reduced by $Ti^{III}$ at low pH (see earlier). At pH ≥ 10, the allyl radical **13** was detected: this may be formed *via* direct hydrogen abstraction by $O^{-\bullet}$.

(*ii*) *Pyrimidine nucleosides and nucleotides.* The reaction of the nucleoside uridine with •OH at pH *ca.* 7 gave a very characteristic spectrum as shown in Fig. 4 (typical of several uridine derivatives, including 2′-, 3′- and 5′-UMP, as well as cytidine). This is analysed in terms of two major doublets, as indicated. The signals are attributed to the spin-trapped C5-OH and C6-OH adducts: the larger splitting (outside lines) is attributed to the C5-adduct, though the expected nitrogen splitting (possibly small) cannot be unambiguously identified. These results and analysis are in accord with those of Riesz and his co-workers[5] who have also commented on the increase in $a$(β-H) and evident reduction in $a$(β-N) in the C5-OH adduct in uridine compared with uracil. It is also notable that, compared with uracil itself, attack on the C6 position is apparently now favoured: we believe that this may reflect a lower rate of the trapping of the C5-OH adduct in the nucleoside as a result of the bulk of the ribose moiety.

The uridine nucleotides 2′-UMP, 3′-UMP and 5′-UMP behaved in an essentially similar manner in the pH range 1–9, though extra peaks in the centre of the spectra for both 2′-UMP and 5′-UMP [Fig. 4(*c*)] may indicate the formation of sugar-derived radicals (for discussion of mechanisms, see below). The spectra from thymidine also showed both C5- and C6-OH adducts (the former with a clear β-nitrogen splitting) at pH *ca.* 7, with only the former observed at low pH (see earlier).

Compared with the spectra of nitroxides derived from related adducts from •OH and, *e.g.*, uridine and 5′-UMP which were separated by HPLC before EPR study,[6–8] our 5′-UMP spectra are generally much more intense (the loss of intensity on

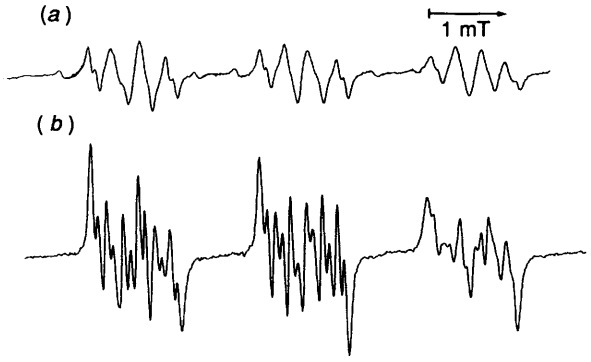


**Fig. 2** (*a*) EPR spectrum of the spin adduct **8** obtained from the addition of the C5-hydroxyl adduct of 1-methylcytosine to MNP at pH 9 [$Ti^{III}$ ($3 \times 10^{-4}$ mol $dm^{-3}$), $H_2O_2$ ($7 \times 10^{-3}$ mol $dm^{-3}$), 1-methylcytosine (0.033 mol $dm^{-3}$), MNP ($2 \times 10^{-2}$ mol $dm^{-3}$)]; (*b*) EPR spectrum of the protonated spin-adduct **9** obtained from ·OH, 1-methylcytosine and MNP at pH 1 [conditions otherwise as Fig. 2(*a*)]

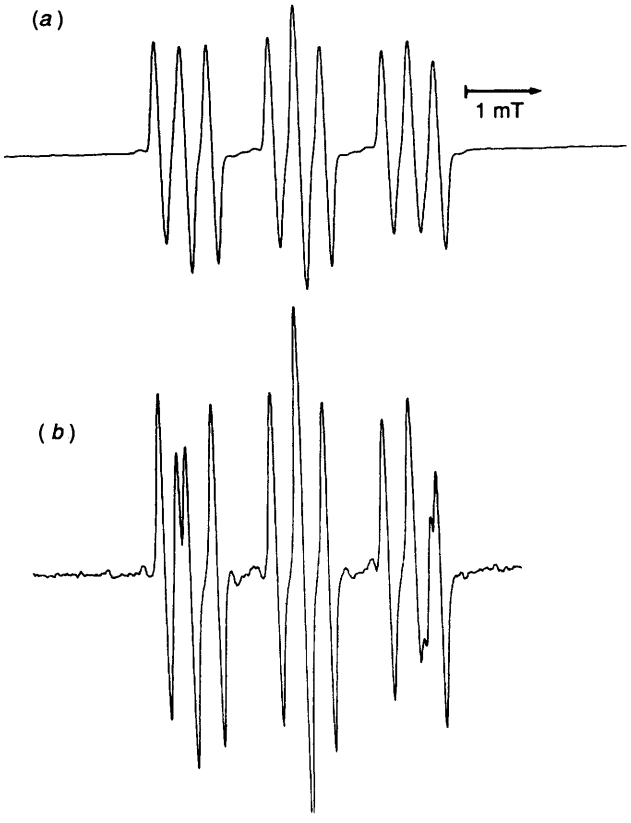


**Fig. 3** (*a*) EPR spectrum of the spin adduct **11** obtained from the addition of the C5-hydroxyl adduct of thymine to MNP at pH 2 [$Ti^{III}$ ($3 \times 10^{-4}$ mol $dm^{-3}$), $H_2O_2$ ($7 \times 10^{-3}$ mol $dm^{-3}$), thymine (0.035 mol $dm^{-3}$), MNP ($2 \times 10^{-2}$ mol $dm^{-3}$)]; (*b*) EPR spectra of the spin-trapped thymine ·OH adducts **11** and **12** at pH 7 [conditions otherwise as Fig. 3(*a*)]

treatment for HPLC has been noted). However, where direct comparison is possible the observation here of dominant doublets (as with uridine or 5′-UMP) corresponds to the major radicals apparent in the earlier studies.

The results described above also establish a uniformity of behaviour of the pyrimidine bases and derivatives—apparently exclusive attack on the reactive C5–C6 double bond. There is no unambiguous evidence for direct attack on sugar moieties or for rapid fragmentation of first-formed base radicals in the majority of cases, even under conditions (*e.g.*, at low pH) where fragmentation might be expected following transfer of damage from pyrimidine radical-cation to sugar (see Scheme 1). This

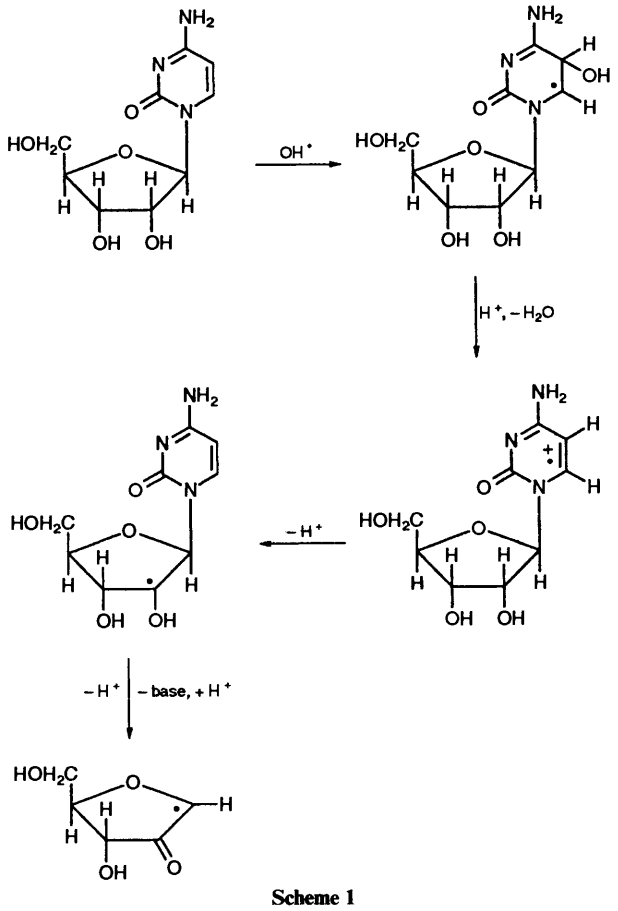


**Scheme 1**

may reflect either the efficiency of the spin-trapping reaction of first-formed radicals (at least at the concentration of spin trap needed for radical detection) or the relative inefficiency of trapping of sugar radicals.

(*b*) *Hydroxyl-radical Attack on Dinucleotides and Polynucleotides.*—We next extended our study to some dinucleotides and, especially, the homopolymer poly(U). It has previously been shown that strand-breakage can be detected following ·OH attack on poly(U)[15] and it has been suggested that sugar–phosphate fragmentation follows reaction of hydroxyl at C5 and C6 in the base (possibly *via* subsequent hydrogen-abstraction from the sugar moiety). A faster acid-catalysed process may involve formation of the base's radical-cation (*via* loss of water from the hydroxyl adducts) as also noted by us in rapid-flow EPR experiments on cytidine[13] (see Scheme 1). Hildenbrand and Schulte-Frohlinde have detected ·OH adducts and a 2′-oxo-3′-yl sugar radical in direct photolysis experiments with poly(U)[16] which suggests that the C2′ sugar radical may readily lose phosphate (as well as the free base), as indicated in Scheme 2.

To seek further evidence for sugar-to-base hydrogen-transfer mechanisms involving neighbouring nucleotides we studied the reactions of ·OH with uridyluridine and thymidylthymidine. In both cases weak EPR spectra of spin-trapped C5-OH-adducts (*cf.* Table 1) were detected over a wide pH range; there was no evidence to suggest the formation of sugar radicals.

However, experiments on poly(U) with $Ti^{III}$–$H_2O_2$ showed a marked pH dependence. Thus in the pH range 2–4, a very broad anisotropic aminoxyl spectrum was obtained, typical of a large, relatively immobile aminoxyl [see, *e.g.*, Fig. 5(*a*)]. When the experiment was repeated at pH 1, an additional much sharper, isotropic spectrum was obtained which is virtually identical with the spectrum from uracil itself [Fig. 5(*b*)]: this provides

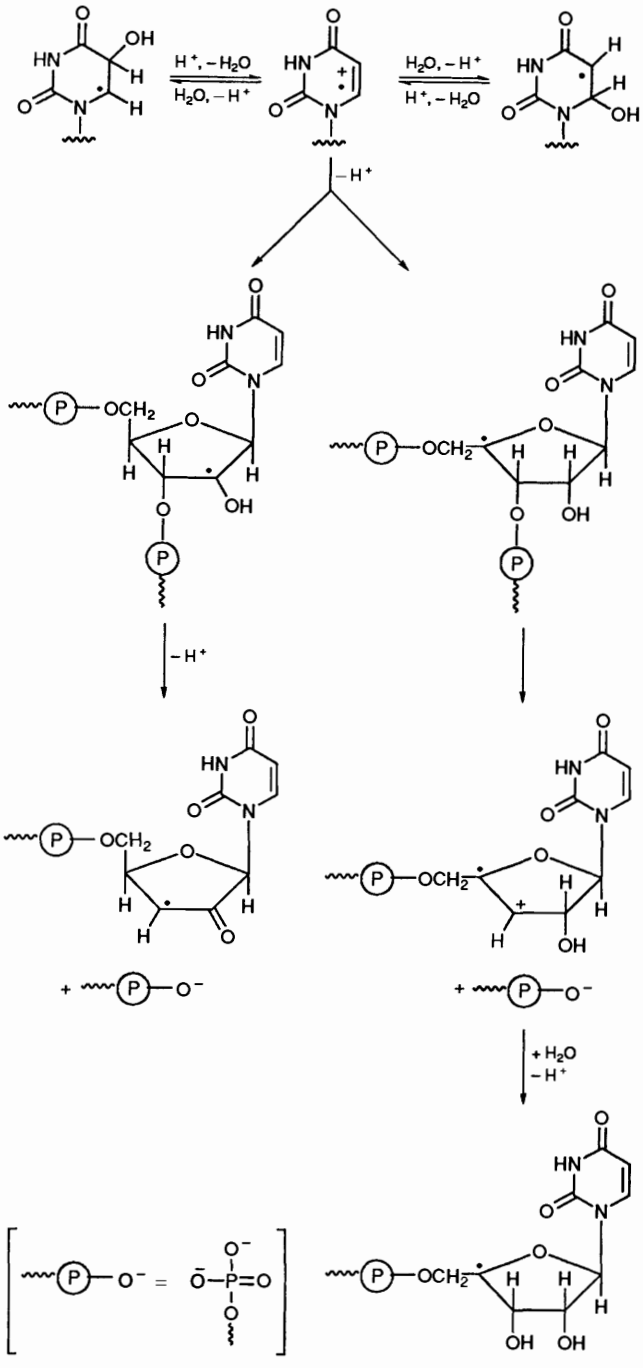

Scheme 2

clear evidence either for strand-breakage to release a small fragment retaining the hydroxyl-radical trapped as an adduct of C5 in the uridine ring or for base-loss, to give uracil, which is attacked by ·OH. At pH 7 a *relatively* mobile spectrum of a similar C5-hydroxyl–uridine adduct was obtained [see Fig. 5(*c*)]. Enzymatic cleavage experiments at pH *ca.* 7 with RNase (see later) also brought about rapid production of a mobile spectrum of the C5-adduct, as expected if the chain is readily cleaved. Background experiments also established that when radical damage and trapping experiments at pH *ca.* 2 [*cf.* Fig. 5(*a*)] was *followed* by change of pH, weaker, ill-resolved but essentially isotropic spectra of uridine-type adducts were obtained at pH 1 and also $\geqslant 7$. This implies that acid- or base-induced cleavage (presumably non-radical) of the trapped aminoxyl adducts themselves cannot be entirely discounted as *contributing* towards the changes noted.

Experiments with $Fe^{II}$–$H_2O_2$ and poly(U) gave results which

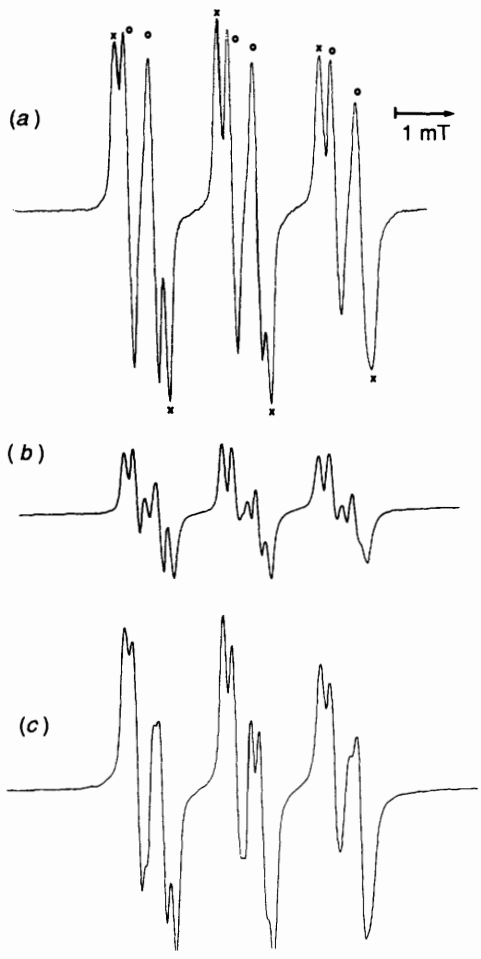


**Fig. 4** (*a*) EPR spectra of the spin adducts of MNP with the C5- and C6-hydroxyl adducts of uridine at pH 7; (*b*) spin adducts from ·OH and uridine at pH 1; (*c*) spin adducts from ·OH and 5′-UMP at pH 7 [$Ti^{III}$ ($3 \times 10^{-4}$ mol $dm^{-3}$), $H_2O_2$ ($7 \times 10^{-3}$ mol $dm^{-3}$), 5′-UMP (0.02 mol $dm^{-3}$), MNP ($2 \times 10^{-2}$ mol $dm^{-3}$)

differed in one important respect from those with $Ti^{III}$: at pH *ca.* 2.5, even with very low concentrations of $Fe^{II}$ (down to $6 \times 10^{-5}$ mol $dm^{-3}$) the spectra of uridine-type adducts obtained were essentially isotropic in nature [*cf.* Fig. 5(*c*)]: in all other respects the spectra observed resembled those from the titanium system. We conclude that a much greater extent of fragmentation is induced by $Fe^{II}$–$H_2O_2$ at pH 2.5 than for $Ti^{III}$–$H_2O_2$. This may reflect a much greater flux of hydroxyl-radical generation [*e.g.*, *via* production of a poly(U)–$Fe^{II}$ complex], a greater selectivity of attack on the sugar (possibly *via* site-selective attack following complexation) or the occurrence of non-radical fragmentation following oxidation of first-formed radicals by $Fe^{III}$.

Experiments were also conducted with poly(C), poly(A), poly(G) and poly(A)·poly(U), under similar conditions; as with poly(U), the $Fe^{II}$–$H_2O_2$ system gave stronger spectra, and this was the method largely employed. At pH 7 poly(C) gave spectra (isotropic but broadened), closely resembling those from cytidine itself and from poly(U) under similar circumstances [see Fig. 5(*c*)]; the spectra became much sharper and more isotropic on treatment wih RNase (see also Fig. 5). On the other hand, under these conditions poly(G) and poly(A) gave very weak, extremely anisotropic spectra from which no base-adducts could be identified (or released with RNase). Poly(A)·poly(U) behaved similarly in that it provided little direct evidence for effective ·OH attack (as might be expected for this double-stranded nucleic acid); but treatment of the solution with RNase caused the appearance of an isotropic

spectrum identical with that from poly(U) (Fig. 5), showing that attack on uridine moieties and subsequent enzymatic release had occurred.

(*c*) *Hydroxyl Radical Attack on RNA.*—When samples of RNA [Sigma: Type VI (pfs), with concentrations typically in the range 5–15 mg $cm^{-3}$] were exposed to •OH attack (from the $Fe^{II}$–EDTA and $Ti^{III}$–$H_2O_2$ couples) at pH 7 under conditions similar to those described earlier and in the presence of the trap MNP (typically $10^{-2}$ mol $dm^{-3}$) weak spectra were observed with a characteristically broadened high-field peak (with traces of a very broad absorption from an immobilized aminoxyl at low field). Stronger spectra were obtained at higher concentrations of hydrogen peroxide. Fig. 6(*a*) shows the spectrum observed with [$Fe^{II}$–EDTA] $5 \times 10^{-4}$ mol $dm^{-3}$, [$H_2O_2$] $5 \times 10^{-4}$ mol $dm^{-3}$. Similar spectra were also observed using other transition metal–hydrogen peroxide couples, including $Cu^{II}$ (typically $10^{-3}$ mol $dm^{-3}$) and $VO^{2+}$ (also $10^{-3}$ mol $dm^{-3}$: *cf.* ref. 17), in each case with [$H_2O_2$] millimolar. The relative intensity was in the order $Fe^{II} > VO^{2+} > Ti^{III} > Cu^{II}$.

On increasing the flux of hydroxyl radicals significantly (*e.g.*, with [$Fe^{II}$] and [$H_2O_2$] both *ca.* $2 \times 10^{-3}$ mol $dm^{-3}$ or greater) the spectra of the trapped radical(s) show an increased resolution and signal height: the clear isotropic spectrum characteristic of a mixture of two triplets of doublets becomes identifiable [see Fig. 6(*b*)]. This resembles the uridine and cytidine adducts discussed above and establishes not only that •OH attack occurs predominantly at the base's double bond in uridine (as noted in Carmichael[17] for the vanadyl-induced Fenton reaction, though his detailed analysis differs from that given here) and/or cytidine, but also that radical-induced fragmentation has occurred. We believe that this process corresponds to fragmentation of the RNA chain in the spin-trapped polymer obtained following initial attack (*i.e.*, that the aminoxyl serves as a spin-label in the polymer chain). Support for this assertion was also obtained by treating the initial adduct produced at low concentrations of iron and hydrogen peroxide with the enzyme RNase: enzymatic digestion leads to rapid conversion of the broadened spectrum [Fig. 6(*a*)] into a sharper spectrum largely characteristic of smaller, trapped RNA fragments [Fig. 6(*c*)]. From this we can identify sites of initial •OH attack as C5 and C6 in the base, though evidence for a third adduct in the centre of the spectrum is also obtained.

Experiments in the absence of oxygen and also with the fully deuteriated spin trap [$^2H_9$]$Me_3CNO$ allowed a small but not significant improvement in spectrum resolution to be obtained, without significantly changing the conclusions.

Further experiments were carried out on samples of RNA which were better defined. For tRNA (Sigma, Type XX from *E. Coli*, Strain W, *M ca.* 25 000) we found that at pH 7, even with higher concentrations of iron and peroxide, the spectrum obtained showed much greater anisotropy (see Fig. 7) with an appearance close to that observed from •OH and poly(U) at pH *ca.* 4 in the presence of low concentrations of $Ti^{III}$ and $H_2O_2$. For the spectrum shown in Fig. 7 we can conclude that a much larger, less mobile radical has been trapped. These observations suggest that tRNA is relatively resistant to •OH-induced fragmentation (even from $Fe^{II}$–$H_2O_2$) compared with poly(U) and poly(C) and with the ill-defined RNA samples investigated earlier. This is believed to reflect the fact that a large proportion of the molecule exists in a double-stranded form [see **32**][18] in which base-attack may be hindered and from which radicals with greatly restricted flexibility might be expected [as also with poly(A)•poly(U)]. Enzymatic degradation gave sharp spectra of C5- and C6-hydroxyl-adducts of uridine, as described above.

Finally, with ribosomal RNA (rRNA Sigma, from *E. Coli*, Strain W) relatively sharp isotropic spectra were obtained upon

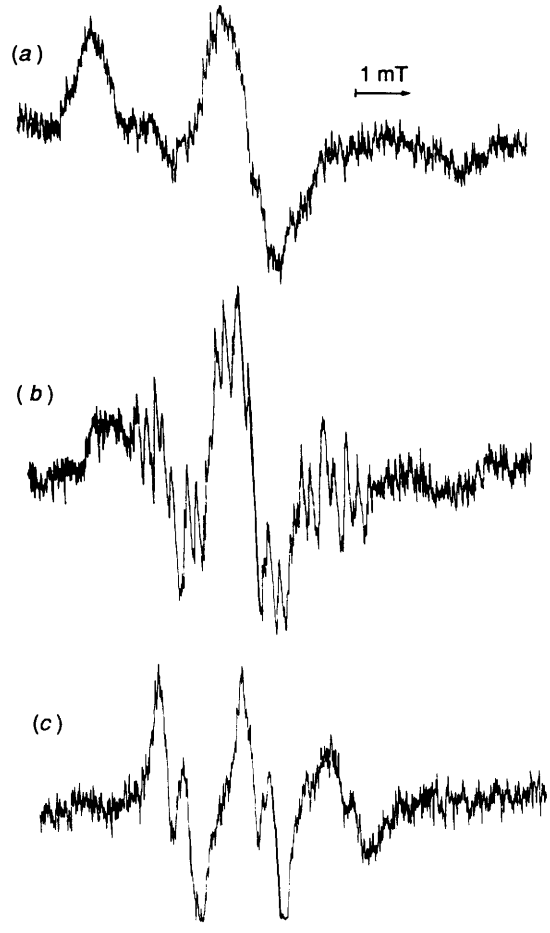


**Fig. 5** (*a*) EPR spectrum of an immobilized aminoxyl formed in the reaction between •OH and poly(U) in the presence of MNP at pH 2.5 [$Ti^{III}$ ($3 \times 10^{-4}$ mol $dm^{-3}$), $H_2O_2$ ($7 \times 10^{-3}$ mol $dm^{-3}$), poly(U) (2 mg $cm^{-3}$), MNP ($2 \times 10^{-2}$ mol $dm^{-3}$)]; (*b*) as (*a*) but at pH 1; (*c*) as (*a*) but at pH 7

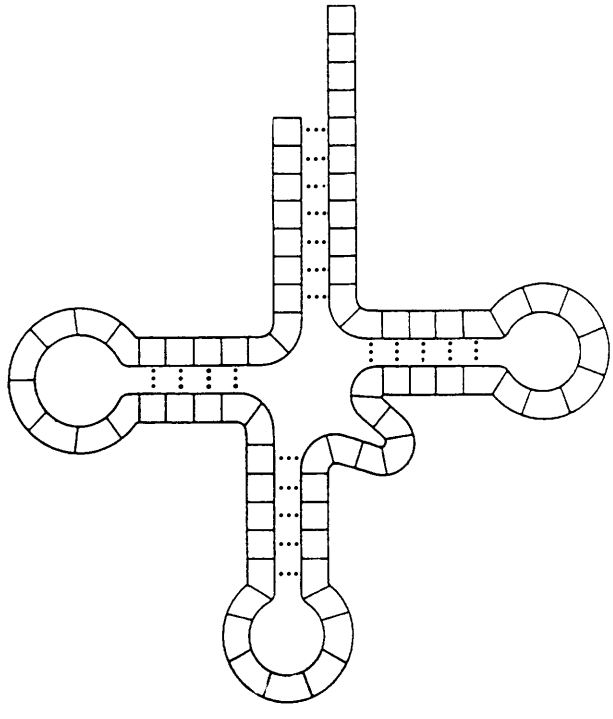

**32**

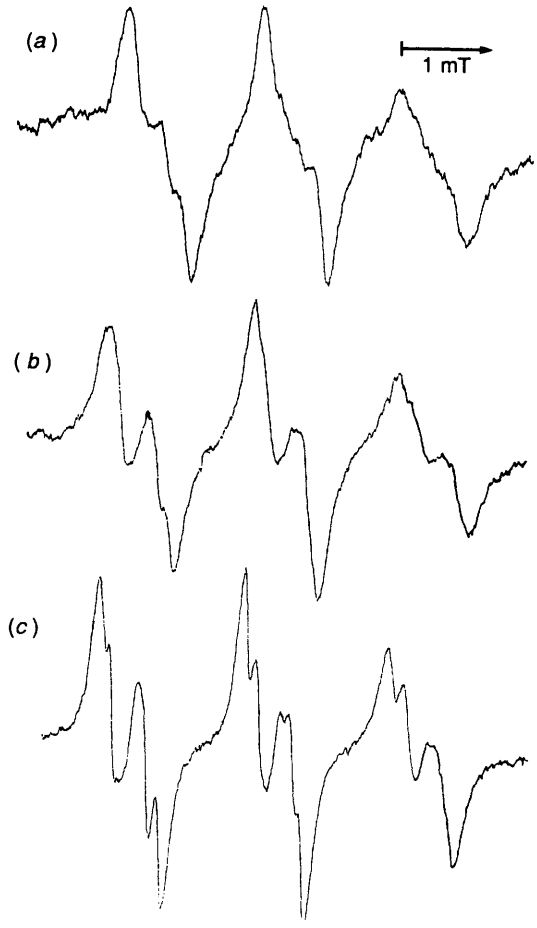


**Fig. 6** EPR spectra from ·OH and RNA (16 mg $cm^{-3}$) in aqueous solution at pH 7: (*a*) $Fe^{II}$–EDTA (5 × $10^{-4}$ mol $dm^{-3}$), $H_2O_2$ (5 × $10^{-4}$ mol $dm^{-3}$), MNP ($10^{-2}$ mol $dm^{-3}$); (*b*) $Fe^{II}$–EDTA (2 × $10^{-3}$ mol $dm^{-3}$), $H_2O_2$ ($10^{-3}$ mol $dm^{-3}$); MNP ($10^{-2}$ mol $dm^{-3}$); (*c*) as (*a*), following addition of RNase (2 mg $cm^{-3}$)

reaction with ·OH: this is as expected, as the sample is believed to be a mixture of three different subunits of rRNA with a range of molecular weights.

## Conclusions

Spin-trapping EPR experiments confirm that free-radical-induced damage to polynucleotides and RNA, brought about by several metal ion–peroxide redox couples, involves attack of ·OH on the C5–C6 double bond in the pyrimidine base; in RNA itself, clear evidence is obtained that attack occurs predominantly at the uridine and cytidine moieties.

Differences in the appearance of the spectra, and comparison with those obtained after enzymatic digestion, can be used to characterize not only the site(s) of attack but also the occurrence of fragmentation (strand-breakage) following prolonged exposure to radicals: it is believed that loss of phosphate from the C2′-sugar derived radicals is involved (see Scheme 2). Differences between pH *ca.* 2 and the greater fragmentation evident at pH 7 [*e.g.*, for poly(U)] may well reflect an enhancement in the rate of hydroxyl-radical formation from the complexed metal ion (possibly bonded to the nucleic acid itself under these conditions). On the other hand the observation of monomeric uracil adducts following radical attack at low pH suggests the occurrence of free-base loss following acid-catalysed transfer of damage from the radical centre at C6 (or radical-cation) to C2′ (see Scheme 1). The crucial role of the pyrimidine and the C2′-oxygen in transfer of damage from the base to the sugar (with subsequent breakdown) is entirely

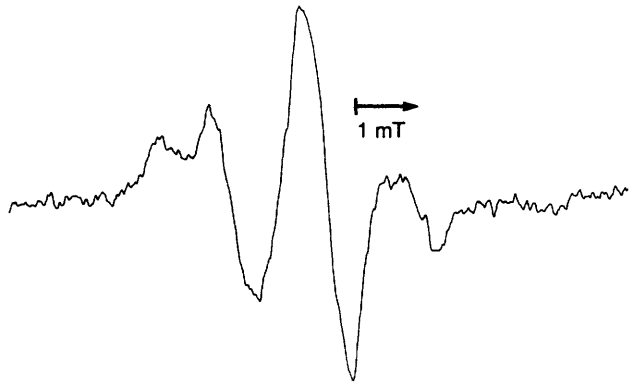


**Fig. 7** EPR spectrum of immobilized aminoxyls obtained from reaction of ·OH with tRNA (*M* 25 000: 16 mg $cm^{-3}$) at pH 7. $Fe^{II}$–EDTA ($10^{-3}$ mol $dm^{-3}$), $H_2O_2$ (2 × $10^{-3}$ mol $dm^{-3}$), MNP ($10^{-2}$ mol $dm^{-3}$).

consistent with the observations that radiation-induced strand-breaks are much more efficient for poly(U) compared with poly(dU)[19] and for poly(U) compared with poly(A).[20]

## Experimental

Experiments were carried out on a Bruker ESP 300 and a JEOL RE1X EPR spectrometer, using an aqueous solution sample cell. In experiments with the pyrimidine bases, nucleosides, and nucleotides, samples were prepared by mixing aqueous solutions of the substrate, MNP, $H_2O_2$ and $Ti^{III}$ (added in that order) to give final concentrations of *ca.* 0.03 mol $dm^{-3}$ (substrate), 2 × $10^{-2}$ mol $dm^{-3}$ (MNP), 7 × $10^{-3}$ mol $dm^{-3}$ ($H_2O_2$) and 3 × $10^{-4}$ mol $dm^{-3}$ ($Ti^{III}$); the MNP solution contained some acetonitrile (having been left to stir for 1–2 h to bring about dissolution of the trap), and EDTA (equivalent to the titanium concentration) was then added in experiments at final pH values >3 (adjusted with $H_2SO_4$ or $NH_3$ as appropriate, before addition of $Ti^{III}$).

In experiments with RNA and polynucleotides (the majority of which involved the use of $Fe^{II}$–EDTA), the spin-trap MNP was also dissolved in aqueous acetonitrile (as above). Solutions of RNA (Sigma, Type VI, Torula Yeast), tRNA (Sigma, Type X, *E. Coli*, Strain W) and rRNA (Sigma, *E. Coli*, Strain W) were prepared in phosphate buffer at pH 7. Solution of the polynucleotides poly(C), poly(G), poly(U) (all potassium salts) and the double-stranded homopolymer poly(A)·poly(U) (sodium salt) (all Sigma) were prepared in phosphate buffer at pH 7 and in some cases in HCl–glycine buffer at pH 2.5. Samples were prepared by combining a mixture of MNP and $H_2O_2$ with a mixture of the substrate and the metal, immediately prior to EPR examination. Concentration of reactants in the final sample were typically 5–15 mg $cm^{-3}$ (substrate), $10^{-2}$ mol $dm^{-3}$ MNP, 5 × $10^{-4}$ to 2 × $10^{-3}$ mol $dm^{-3}$ ($Fe^{II}$–EDTA and $H_2O_2$), with *ca.* 10% acetonitrile. Enzymatic digestion of the adduct with RNase (type 1-AS, bovine pancreas) was performed at 37 °C for between 30 and 60 min; typically 2 mg $cm^{-3}$ of RNase was added to the final solution after mixing. Before and during mixing, solutions for EPR experiments were normally purged with nitrogen.

All chemicals were samples obtained from commercial sources (nucleotides and their derivatives from Sigma), used without further purification.

## Acknowledgements

We thank both the SERC and AICR for their financial support (for studentships and contributions towards purchase of the EPR spectrometers).

## References


1 C. von Sonntag, *Radiat. Phys. Chem.*, 1987, **30**, 313 (*Int. J. Radiat. Appl. Instrum. Part C*).
2 G. Scholes in *Effects of Ionizing Radiation on DNA*, eds. A. J. Bertinchamps, J. Hütterman, W. Köhnlein and R. Teoule, Springer-Verlag, Berlin, 1973, 153.
3 M. J. Burkitt, M. Fitchett and B. C. Gilbert in *Medical, Biochemical and Chemical Aspects of Free Radicals*, eds. O. Hayaishi, E. Niki, M. Kondo and T. Yoshigawa, Elsevier, Amsterdam, 1988, p. 63.
4 D. Schulte-Frohlinde and K. Hildenbrand in *Free Radicals in Synthesis and Biology*, ed. F. Minisci, NATO ASI series, Kluwer, Dordrecht, 1989, 335.
5 P. Riesz and S. Rustgi, *Radiat. Phys. Chem.*, 1979, **13**, 21.
6 O. Inanami, M. Kuwabara and F. Sato, *Radiat. Res.*, 1987, **112**, 36.
7 O. Inanami, M. Kuwabara, D. Endoh and F. Sato, *Radiat. Res.*, 1986, **108**, 1.
8 S. Kominami, S. Rokushika and H. Hatano, *Int. J. Radiat. Biol.*, 1976, **30**, 525.
9 M. Al-Sheikhly and C. von Sonntag, *Z. Naturforsch., Teil B*, 1983, **38**, 1622.
10 M. Dizdaroglu and M. G. Simic, *Int. J. Radiat. Biol.*, 1984, **46**, 241.
11 G. A. Infanta, P. Jirathana, J. H. Fendler and E. J. Fendler, *J. Chem. Soc., Faraday Trans. 1*, 1973, **69**, 1586.
12 C. von Sonntag, *The Chemical Basis of Radiation Biology*, Taylor and Francis, London, 1987.
13 H. Catterall, M. J. Davies and B. C. Gilbert, *J. Chem. Soc., Perkin Trans. 2*, 1992, 1379.
14 P. O. Ts'O in *Basic Principles in Nucleic Acid Chemistry*, Academic Press, New York and London, 1974, 462.
15 D. G. E. Lemaire, E. Bothe and D. Schulte-Frohlinde, *Int. J. Radiat. Biol.*, 1984, **45**, 351.
16 K. Hildenbrand and D. Schulte-Frohlinde, *Int. J. Radiat. Biol.*, 1989, **55**, 725.
17 A. J. Carmichael, *FEBS Lett.*, 1990, **261**, 165.
18 *Transfer RNA*, ed. S. Altman, MIT Press, Cambridge, MA, and London.
19 E. Hankiewicz, E. Bothe and D. Schulte-Frohlinde, *Free Radical Res. Commun.*, 1992, **16**, 391.
20 C. P. Murthy, D. J. Deeble and C. von Sonntag, *Z. Naturforsch., Teil C*, 1988, **43**, 572.


*Paper* 3/01968C
*Received* 30*th March* 1993
*Accepted* 20*th April* 1993